

Evidence for the Coexistence of Anisotropic Superconducting Gap and Nonlocal Effects in the Non-magnetic Superconductor $\text{LuNi}_2\text{B}_2\text{C}$

Tuson Park¹, Elbert E. M. Chia², M. B. Salamon², E. D. Bauer¹, I. Vekhter¹, J. D. Thompson¹, Eun Mi Choi³, Heon Jung Kim³, Sung-Ik Lee³, and P. C. Canfield⁴

¹Los Alamos National Laboratory, Los Alamos, New Mexico 87545

²Department of Physics and Material Research Laboratory,
University of Illinois at Urbana-Champaign, IL 61801, USA

³National Creative Research Initiative Center for Superconductivity and Department of Physics,
Pohang University of Science and Technology, Pohang 790-784, Republic of Korea

⁴Ames Laboratory, Department of Physics and Astronomy, Iowa State University, Ames, Iowa 50011
(Dated: March 22, 2024)

A study of the dependence of the heat capacity $C_p(\theta)$ on field angle in $\text{LuNi}_2\text{B}_2\text{C}$ reveals an anomalous disorder effect. For pure samples, $C_p(\theta)$ exhibits a fourfold variation as the field $H < H_{c2}$ is rotated in the $[001]$ plane, with minima along $\langle 100 \rangle$ ($\theta = 0$). A slightly disordered sample, however, develops anomalous secondary minima along $\langle 110 \rangle$ for $\mu_0 H > 1$ T, leading to an 8-fold pattern at 2 K and 1.5 T. The anomalous pattern is discussed in terms of coexisting superconducting gap anisotropy and non-local effects.

Exotic superconductors, defined as those that follow the Uemura relation [1] between the superconducting transition temperature T_c and the magnetic penetration depth λ , T_c / λ^2 , have physical properties that differ from conventional (BCS) superconductors. High- T_c cuprates, bismuthates, Chevrel-phases, organic, and heavy-fermion superconductors were suggested to constitute this class. For most of the members, the superconducting gap function is highly anisotropic or has gap zeros on the Fermi surface [2]. The rare-earth nickelborocarbides $\text{RNi}_2\text{B}_2\text{C}$ ($R = \text{Y}, \text{Lu}, \text{Tm}, \text{Er}, \text{Ho}, \text{and Dy}$) remain a challenge because they share many features in common with the exotic superconductors but, like elemental BCS superconductors, fall below the Uemura trend [3].

Unlike BCS superconductors, which exhibit exponential temperature dependence in density-of-states (DOS)-dependent quantities below T_c , the borocarbides have power-law temperature dependences in their low temperature specific heat [4], NMR $1/T_1$ [5], and thermal conductivity [6], indicating that electronic excitations persist even well below T_c . Recently, compelling evidence for the presence of nodes along $\langle 100 \rangle$ directions has been reported both from field-angle thermal conductivity [7] and field-angle heat capacity measurements [8] of $\text{YNi}_2\text{B}_2\text{C}$.

Another interesting feature of the borocarbides is that the flux-line lattice (FLL) undergoes a field-driven transition from hexagonal to square with increasing magnetic field H_k [001] [9, 10, 11]. Kogan et al. successfully incorporated nonlocal corrections to the London model and Fermi surface anisotropy in these materials [12] to describe the transition within a BCS scheme, i.e., isotropic s-wave gap with electron-phonon coupling. Nonlocal effects were also used to explain, without resorting to any exotic order parameter, the modulation of the upper critical field $H_{c2}(\theta)$ [13] and magnetization $M(\theta)$ [14] with the angle between the magnetic field and the crystal

axes. The two seemingly irreconcilable viewpoints have only increased the confusion about the nature of the order parameter of the borocarbides. Recently, Nakai et al. considered the coexistence of an anisotropic gap and nonlocal effects in the borocarbides [15] and thereby explained the reentrant FLL transformation [16] in terms of the interplay between the two effects. In this report, we present further evidence for the coexistence of the gap anisotropy and nonlocal effects. In clean systems, the gap anisotropy effects dominate while both effects are comparable in less clean samples.

Single crystals of $\text{LuNi}_2\text{B}_2\text{C}$ were grown in a Ni_2B flux as described elsewhere [17]. Samples A and C were not annealed while sample N was annealed at $T = 1000$ C for 100 hours under high vacuum. Typical sample dimensions were $1 \times 1 \times 0.1$ mm³. The crystal axes of the sample were determined by two independent methods, x-ray and upper critical field measurements as a function of magnetic field angle [13], which were consistent with each other. The T_c 's, determined by the point where the steepest drop occurs in the resistive superconducting transition, are 15.5, 15.9, and 16.1 K for sample A, C and N respectively (not shown). The resistivity at T_c is 2.34 and 1.44 $\mu\Omega$ cm for sample A and sample N, corresponding to mean free paths of 144.5 and 234 Å respectively. Assuming that 16.1 K is the transition temperature for a pure sample, sample A with T_c of 15.5 K is equivalent to 0.8 % of Co doping on the Ni site, i.e., $\text{Lu}(\text{Ni}_{1-x}\text{Co}_x)_2\text{B}_2\text{C}$ with $x = 0.008$ [18]. The disorder in sample A may be associated with defects which can be removed by judicious post growth annealing [19].

Using an ac technique [8], we have measured the low temperature specific heat of non-magnetic $\text{LuNi}_2\text{B}_2\text{C}$ as a function of magnetic field intensity and magnetic field angle. Three samples of $\text{LuNi}_2\text{B}_2\text{C}$ with different T_c 's, labeled A, C, and N, were studied and revealed an anomalous disorder effect. The heat capacity of the samples

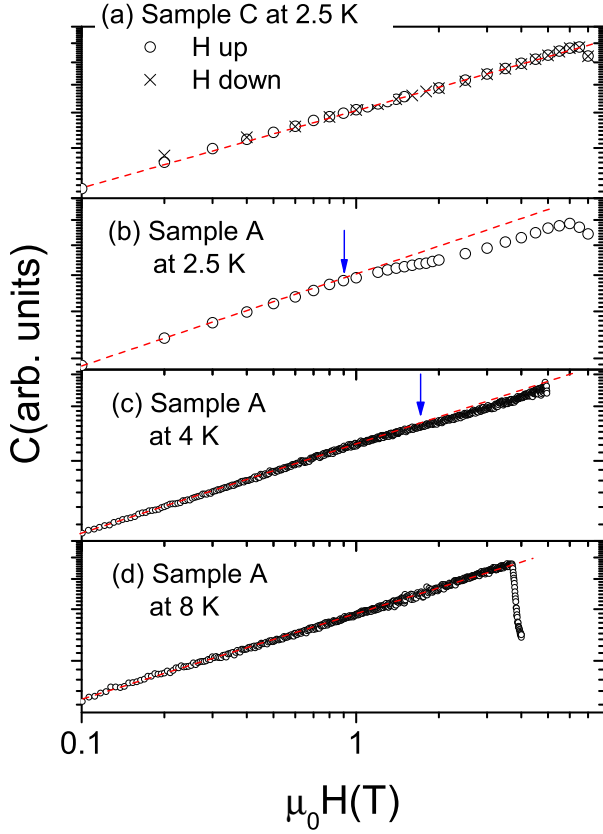


FIG. 1: (a) Heat capacity of sample C at 2.5 K for $H \parallel [110]$. (b)–(d) Heat capacity of sample A at 2.5, 4, and 8 K, respectively for $H \parallel [110]$. Dashed lines are $H^{1/2}$ fit and arrows indicate the deviation point from $H^{1/2}$.

with higher T_c 's shows a fourfold pattern as a function of magnetic field angle, confirming the result from the other non-magnetic borocarbide YNi_2B_2C that the superconducting gap is highly anisotropic with nodes along $\langle 100 \rangle$ [8]. In contrast, the heat capacity of the disordered sample with the lowest T_c (sample A) shows a dramatic change in the field-angle heat capacity above 0.8 T at 2 K: the maxima along $\langle 110 \rangle$ split, giving rise to minima separated by $\phi = 4$ (eightfold pattern) and, further, C_p deviates from a square-root field dependence at the same field, labeled H_{s1} . The eightfold pattern and the deviation from $H^{1/2}$ dependence in sample A are consistent with the coexistence of an anisotropic gap and nonlocal effects.

Fig. 1(a) shows the magnetic field dependence of the heat capacity of sample C at 2.5 K with increasing (circles) and decreasing (crosses) magnetic field. The dashed line represents the least-square fit of $C_0 + b(H - H_0)^{1/2}$, where C_0 is zero-field heat capacity and $H_0 = 0.1$ T is a fitting parameter that takes account of the Meissner effect. The best fit is obtained when $b = 0.46$, namely the Volovik effect for nodal superconductors [20, 21], and is consistent with previous reports on the non-magnetic

borocarbides [4]. Fig. 1(b), (c), and (d) show the heat capacity of sample A at 2.5 K, 4 K, and 8 K, respectively. The dashed line is the square-root field dependence and the arrows indicate where the data deviate from the fit. The deviation field shows systematic increase with temperature, i.e., 0.8 T at 2.5 K, 1.8 T at 4 K, and no clear deviation at 8 K. Above the deviation field, the data fall below the $H^{1/2}$ line.

Field-angle heat capacity directly measures the change in the DOS with magnetic field direction. The DOS of a d-wave superconductor has been shown to exhibit a fourfold oscillation with field angle against crystal axes [22]. At $T = 0$ K, the DOS has a simple form:

$$N(E; H; \phi) = N_0 D_4 (1 + \phi \sin 2\phi); \quad (1)$$

where D_4 is a Doppler-shift induced coefficient and describes the oscillation amplitude. The field-angle sensitive Doppler effect, arising from the supercurrent flows circulating around the vortices, leads to maxima in the DOS when field is along gap maxima and DOS minima when field is along nodes. A 3D superconductor has a much reduced oscillation amplitude ($\sim 6\%$) compared to that of a 2D system ($\sim 40\%$) due to contributions from the out-of-plane component. We note that a similar effect is predicted for an (s+g)-wave superconductor [23].

Fig 2(a) and 2(b) show the low-temperature field-angle heat capacity of sample C at 2.5 K and sample A at 2 K, respectively. The samples were field-cooled to 2 K (or 2.5 K) and were rotated within the ab-plane by a computer controlled stepping motor at increments of 3° . The heat capacity with increasing and decreasing field angle showed reversible behavior for all measured fields, indicating that flux pinning effect is negligible in our measurement. Background contributions (C_{bkg}) from lattice vibrations and thermometry were subtracted in the usual manner [8] and the remaining field-induced heat capacity $C = C_{total} - C_{bkg}$ was analyzed in terms of $C(\phi) = c(1 + \phi \sin 2\phi)$ for pure samples. At low fields, there is a clear fourfold oscillation with minima along $\langle 100 \rangle$ for both samples, indicating that the zeros of the gap are located along those directions, consistent with those of YNi_2B_2C [7, 8]. The oscillation amplitude is about 4% for all three samples (sample N is not shown, but is essentially the same as sample C); this is consistent with the 3D superconductivity in the borocarbides [24].

At 1 T, surprisingly, the heat capacity of sample A develops minima along $\langle 110 \rangle$, producing two sets of fourfold patterns or 8-fold, an effect not observed in either sample C or sample N with higher T_c 's. The crossover field from the fourfold to the $(4+4)$ pattern of sample A lies between 0.6 and 1 T, which is also the point where the heat capacity of sample A deviates from the square-root field dependence (see Fig. 1). With increasing field, the splitting in sample A gradually disappears and the field-angle heat capacity recovers its fourfold pattern above

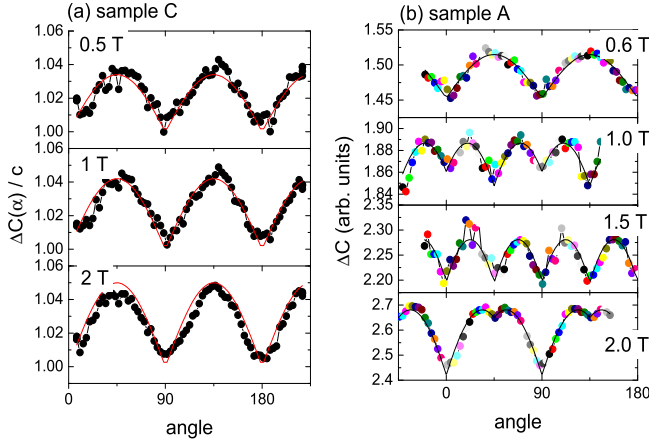


FIG. 2: (a) Normalized heat capacity of sample C at 2.5 K and a 4-fold oscillation (solid line), $C(\alpha) = C(1 + \sin 2\alpha)$. (b) Field-induced heat capacity of sample A at 2 K, $C = C_{\text{total}} - C_{\text{bkg}}$, and a 4+4 pattern (solid line) – see text.

4 T. We also measured the field-angle heat capacity of sample A at 4 K to check if the anomalous peak splitting persists at higher temperatures (not shown). The four-fold pattern now persists to 1 T, evolving into two sets of fourfold patterns above 2 T. The 4 T data at 4 K has a shape similar to the 2 T data at 2 K. The crossover field H_{s1} increases with increasing temperature.

We focus on the fact that the anomalous 8-fold pattern occurs only at sample A which has half the electronic mean free path of the sample N while the T_c is slightly decreased. According to the nonlocal theory by Kogan et al. [12], the hexagonal-to-square FLL transition depends on the electronic mean free path l and the superconducting coherence length of the sample. Gamma et al. found that a mere 9% of Co doping onto the Ni site in Lu1221 can make the FLL transition field at least 20 times higher than that of pure matrix for H k [001] [25]. Because the FLL transition field for pure sample is expected to be small [12] (possibly below our measurement range) the nonlocal effects would not influence the field-angle heat capacity of sample N (or C). In contrast, the disorder in sample A is expected to increase the transition to a higher field, i.e. to a field relevant in the field-angle heat capacity measurement.

When the magnetic field is rotated within ab-plane, the transition field may differ with different field directions because of the different nonlocal range, i.e., $\lambda = 1$. The two different transition fields can be characterized by H_{s1} and H_{s2} . As a magnetic field rotates within the ab-plane for $H_{s1} < H < H_{s2}$, the FLL will experience a structural change (or distortion), i.e. hexagonal for H k [100] and square for H k [110]. Since the borocarbides have nodes on the Fermi surface, the DOS will differ depending on the FLL structure [21]. The negative deviation from the $H^{-1/2}$ above H_{s1} in the heat capacity

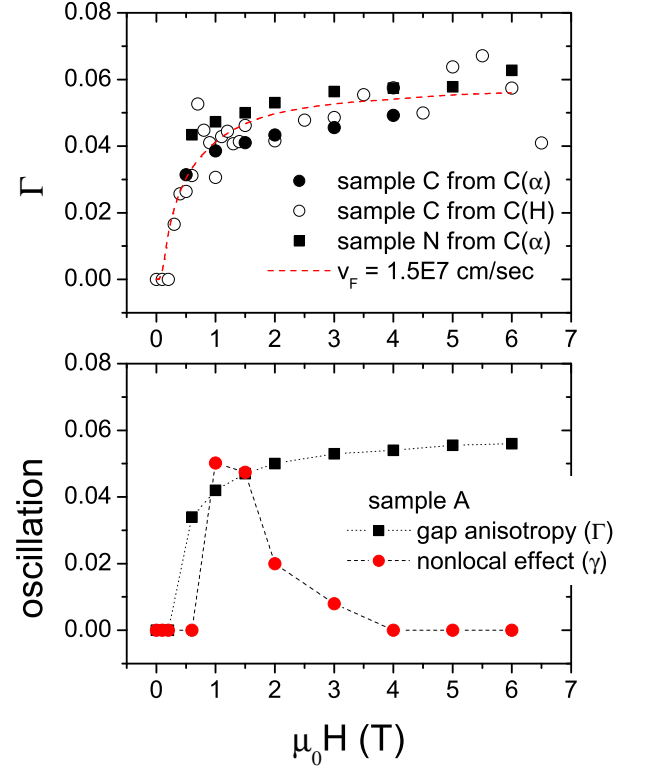


FIG. 3: Oscillation amplitude of sample C (circles) and sample N (squares). The dashed line is from the 3D nodal quasiparticle theory with $v_F = 1.5 \times 10^7$ cm/sec [8]. The bottom panel contrasts the oscillation amplitude due to the nonlocal effect (circles) and gap anisotropy (squares).

of sample A (see Fig. 1b) also indicates that the DOS of the hexagonal FLL is larger than that of the square FLL. The additional FLL anisotropy in the DOS will modulate the gap-anisotropy oscillation and leads to a (4+4)-fold pattern.

We hypothesize that the two effects are independent of each other and have a form of two cusped 4-fold oscillations in the DOS:

$$C(\alpha) = p_1 + p_2(1 + \sin 2\alpha)(1 + \sin 2(\alpha - 45^\circ)); \quad (2)$$

where p_1 and p_2 are fitting parameters. The value represents the oscillation due to gap anisotropy in pure samples (see Fig. 3). The nonlocal effects give rise to a 45°-shifted 4-fold pattern and are accounted for by p_2 . The solid line in Fig. 2 (b) is the least square fit of Eq. (2) and represents the data very well. The oscillations due to the nonlocal effects (γ) and the gap anisotropy (Γ) at 2 K are compared as a function of magnetic field at the bottom panel of Fig. 3. The FLL effect increases sharply above 0.6 T and decreases gradually to zero at 4 T, indicating that the low field corresponds to H_{s1} and the high field to H_{s2} .

Fig. 4 summarizes the H - T phase diagram of the disordered sample A. Unlike pure samples, it has additional

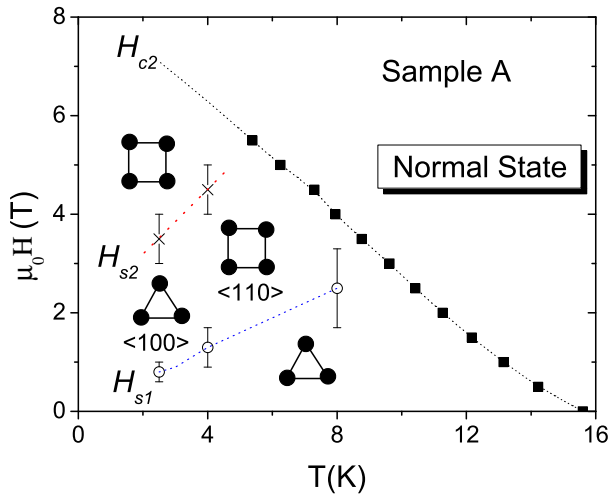


FIG. 4: H - T phase diagram of sample A with lowest T_c . H_{s1} is the FLL transition for $H \parallel [110]$ and H_{s1} for $H \parallel [100]$. The dotted lines are guide to the eye. Triangles and squares were sketched to show the corresponding FLL.

phase lines in the superconducting state where the field-angle heat capacity shows a crossover from fourfold to the $(4+4)$ -pattern (H_{s1}) or vice versa (H_{s2}). The increase in the crossover fields with increasing temperature is consistent with the nonlocal effects [12], adding strength to our viewpoint that the anomalous 8-fold pattern is due to the coexistence of nonlocal effects and gap anisotropy. We note, however, that the difference between the two transition fields H_{s1} and H_{s2} is larger than that expected within the nonlocal theory [12]. For discussion, we assume that the anisotropy in the FLL transition field between $\langle 001 \rangle$ and $\langle 100 \rangle$ is similar to that between $\langle 110 \rangle$ and $\langle 100 \rangle$ because the H_{c2} anisotropy is almost same for the two configurations. The observed ratio $H_{s2}/H_{s1} \approx 4$ is larger than the predicted ratio 2 [12], but is smaller than the reported ratio of 10 in YNi_2B_2C [26]. The difference between experiments and theory may attest that we need to account for both nonlocality and anisotropic gap nature of the borocarbides.

In summary, we have studied the non-magnetic superconductor $LuNi_2B_2C$ via the dependence of heat capacity on magnetic field angle and magnetic field. Unlike pure samples, a slightly disordered sample A shows a deviation from $H^{1/2}$ and a $(4+4)$ -fold pattern in $C_p(T)$ at above 1 K. The anomalous properties were explained in terms of the coexistence of gap anisotropy and nonlocal effects. These experiments resolve the apparently irreconcilably different views on the nature of the order parameter in the non-magnetic borocarbides.

This project was supported in part by NSF Grant No. DMR-99-72087 and at Pohang by the Ministry of Science and Technology of Korea through the Creative Research Initiative Program. This manuscript has been authored by Iowa State University of Science and Technology un-

der Contract No. W-7405-ENG-82 with the U.S. Department of Energy. X-ray measurements were carried out in the Center for Microanalysis of Materials, University of Illinois, which is partially supported by the U.S. Department of Energy under grant DEFG 02-91-ER 45439. We thank S. Baily, N. Moreno-Salazar, and M. Hundley for their help in performing experiments. T. Park and M. Salam acknowledge benefits from the discussion with S. Balatsky, T. Leggett and K. Machida.

Current address: Department of Physics and Astronomy, Louisiana State University, Baton Rouge, LA 70803, USA

- [1] Y. J. Uemura, L. P. Le, G. M. Luke, B. J. Sternlieb, W. D. Wu, J. H. Brewer, T. M. Riseman, C. L. Seaman, M. B. Maple, M. Ishikawa, et al., Phys. Rev. Lett. 66, 2665 (1991).
- [2] J. F. Annett, Physica C 317, 1 (1999).
- [3] B. H. Brandow, Phil. Mag. 83, 2487 (2003), references therein.
- [4] M. Nohara, M. Isshiki, H. Takagi, and R. J. Cava, J. Phys. Soc. Jpn. 66, 1888 (1997).
- [5] G.-Q. Zheng, Y. Wada, K. Hashimoto, Y. Kitaoka, K. Asayama, H. Takeya, and K. Kadowaki, J. Phys. Chem. Solids 59, 2169 (1998).
- [6] E. Boaknin, R. W. Hill, C. Proust, C. Lupien, L. Taillefer, and P. C. Canfield, Phys. Rev. Lett. 87, 237001 (2001).
- [7] K. Izawa, K. Kamata, Y. Nakajima, Y. Matsuda, T. Watanabe, M. Nohara, H. Takagi, P. Thalmeier, and K. Machi, Phys. Rev. Lett. 89, 137006 (2002).
- [8] T. Park, M. B. Salam, E. M. Choi, H. J. Kim, and S.-I. Lee, Phys. Rev. Lett. 90, 177001 (2003).
- [9] Y. Dewilde, M. Iavarone, U. Welp, V. Metlushko, A. E. Koshelev, I. Aranson, G. W. Crabtree, and P. C. Canfield, Phys. Rev. Lett. 78, 4273 (1997).
- [10] M. R. Eskildsen, P. L. Gammel, B. P. Barber, A. P. Ramirez, D. J. Bishop, N. H. Andersen, K. Mortensen, C. A. Bolle, C. M. Lieber, and P. C. Canfield, Phys. Rev. Lett. 79, 487 (1997).
- [11] M. Yethiraj, D. M. Paul, C. V. Tommy, and E. M. Forgan, Phys. Rev. Lett. 78, 4849 (1997).
- [12] V. G. Kogan, M. Bullock, B. Harmon, P. Miranovic, L. Dobrosavljevic-Grujic, P. L. Gammel, and D. J. Bishop, Phys. Rev. B 55, R8693 (1997).
- [13] V. Metlushko, U. Welp, A. Koshelev, I. Aranson, G. W. Crabtree, and P. C. Canfield, Phys. Rev. Lett. 79, 1738 (1997).
- [14] L. Civale, A. V. Silhanek, J. R. Thompson, K. J. Song, C. V. Tommy, and D. M. Paul, Phys. Rev. Lett. 83, 3920 (1999).
- [15] N. Nakai, P. Miranovic, M. Ichioka, and K. Machida, Phys. Rev. Lett. 89, 237004 (2002).
- [16] M. R. Eskildsen, A. B. Abrahamson, V. G. Kogan, P. L. Gammel, K. Mortensen, N. H. Andersen, and P. C. Canfield, Phys. Rev. Lett. 86, 5148 (2001).
- [17] B. K. Cho, P. C. Canfield, L. L. Miller, D. C. Johnston, W. P. Beyermann, and A. Yatskar, Phys. Rev. B 52, 3684 (1995).
- [18] K. O. Cheon, I. R. Fisher, V. G. Kogan, P. C. Canfield,

- P. M. Iordanov, and P. L. Gammel, Phys. Rev. B 58, 6463 (1998).
- [19] X. Y. Miao, S. L. Bud'ko, and P. C. Canfield, J. Alloys Comp. 338, 13 (2002).
- [20] G. E. Volovik, JETP Lett. 58, 469 (1993).
- [21] M. Ichioka, A. Hasegawa, and K. Machida, Phys. Rev. B 59, 184 (1999).
- [22] I. Vekhter, P. J. Hirschfeld, J. P. Carbotte, and E. J. Nicol, Phys. Rev. B 59, R9023 (1999).
- [23] K. Maki, H. Won, P. Thalmeier, Q. Yuan, K. Izawa, and Y. Matsuda, Europhys. Lett. 64, 496 (2003).
- [24] L. F. Mattheiss, Phys. Rev. B 49, 13279 (1994).
- [25] P. L. Gammel, D. J. Bishop, M. R. Eskildsen, K. Mortensen, N. H. Andersen, I. R. Fisher, K. O. Cheon, P. C. Canfield, and V. G. Kogan, Phys. Rev. Lett. 82, 4082 (1999).
- [26] H. Sakata, M. Oosawa, K. Matsuba, N. Nishida, H. Takeya, and K. Hirata, Phys. Rev. Lett. 84, 1583 (2000).